JOURNAL OF MATERIALS SCIENCE 12 (1977) 1857–1861

The fracture toughness of a nickel-aluminium bronze

J. T. BARNBY
Department of Metallurgy and Materials, University of Aston, Birmingham, UK

E. A. CULPAN, M. S. ATHERTON, D. M. RAE
AUWE, Portland, Dorset UK

Critical stress intensity factors for two slightly different compositions of nickel-aluminium bronze were estimated using J-integral testing methods. The material was in cast form and tested as 10 mm thick three-point bend bars. Toughness values were ~125 MN m$^{-3/2}$ and crack tip opening displacements were ~0.3 mm. The crack tip opening displacements were too small to be accurately and reproducibly measured. Specimens tested with 0.2 mm wide spark-machined slits gave equivalent toughness values to specimens pre-fatigue cracked, within experimental error.

1. Introduction

Nickel–aluminium bronze, even in sand cast form, is a high-toughness corrosion-resistant alloy with useful yield strength. Indeed the toughness level is so high that there is great difficulty in its measurement, since normal notched laboratory size test pieces reach general yield before fracture.

General yield fracture mechanics such as the J-integral technique [1] or the crack opening displacement (COD) techniques [2, 3] are appropriate test methods. These methods have been used in the work described below, in which estimates of toughness were made in order to assist optimization of alloy compositions, and in order to provide design data on toughness for the various geometrical configurations in which nickel–aluminium bronze is used, especially that of pressure vessels.

A familiar feature of high-toughness materials is that increases in crack tip sharpness beyond a critical value cease to reduce fracture stresses [4]. If this cut-off radius is within the range of engineering notches, then such notches are not effectively sharpened by fatigue damage. A further objective of the work below was to determine whether fatigue cracks effectively sharpen sharp engineering notches.

2. Experimental materials and methods

2.1. Materials

The bronzes were produced in the form of 50 mm thick sand-cast blocks to two different chemical compositions, both within the specification BS 1400 AB2. The main difference thought to affect mechanical properties was the difference in aluminium content. The chemical compositions of the alloys are shown in Table I.

Specimens cut from the cast blocks were nominally 160 mm long, 10 mm thick (B) and 30 mm wide (W). Central notches were nominally 10 mm deep giving ($W-a$) nominally 20 mm. Each alloy was tested with the final notch tip produced by spark-machining in one set of specimens, whilst a further set had the final 2 mm of notch produced by fatigue cracking in three-point bending. Spark machined tips were 0.2 mm wide. Fatigue pre-cracking was carried out at a ΔK of 25 MN m$^{-3/2}$.

TABLE I Composition of the alloys (wt%)

Alloy	Al	Fe	Ni	Mn	Cu
HA*	9.5	4.5	5.0	1.4	Balance
LA	8.9	4.3	5.0	1.3	Balance

* HA = High aluminium content, LA = Low aluminium content.

2.2 *J*-Integral Methods

J-integral values were calculated from single tests [5] from slow three-point bend tests over a span of 120 mm. The cross-head speed of the test machine was 0.508 mm min^{-1}. An automatic record of load versus load-point displacement was plotted on an $X-Y$ chart. Load point displacement was measured by an electrical transducer pushed downwards by the bottom of the bend specimen. A calibration curve to give the load versus load-point displacement relation for an unnotched specimen was produced experimentally using an identically dimensioned specimen with no notch.

The point of crack initiation was detected by the potential drop technique [6]. A constant current source was used to pass 26 A (at ~0.3 V) along the bend specimen which was electrically insulated from the test rig. Potential probes spaced at 10 mm across the notch on the notched edge gave an initial potential of typically 20 μV as shown in Fig. 1. The stability of the instrumentation was such that a change of 0.5 μV in the potential reproducibly indicated initiation of cracking. When this change was detected the point was marked on the load versus load-point deflection curve.

J-integral values were obtained using [5]

$$J = \frac{2}{B(W-a)} \int_0^{\delta_{\text{crack}}} P \, \mathrm{d}(\delta_{\text{crack}})$$

The integral was evaluated by estimating the area under the load versus load-point displacement curve, to the point of crack initiation, and subtracting the area corresponding to

$$\int_0^{\delta_{\text{no crack}}} P \mathrm{d}(\delta_{\text{no crack}})$$

using the experimental $\delta_{\text{no crack}}$ calibration. The results were then converted to the K_c values using

$$K_c = (EJ_c)^{1/2}$$

As 10 mm thick specimens certainly correspond to plane stress plastic yielding at the crack tip, the Young's modulus, E was taken to the 124 GN m^{-2}.

2.3. Crack opening displacement

In order to avoid extra instrumentation, crack tip opening displacements were obtained by measurement of fiducial markers at the crack tip. Microhardness indentations were made along the spark-machined slots or fatigue cracks. These were photographed before the test with an internal calibration marker in the photograph. Most tests were stopped immediately after initiation was definite. In all cases this event occurred after general yield. The off-load COD at this stage was then measured by re-photographing the crack tips Since initiation was after general yield the difference between on-load and off-load COD is negligible. The photographs gave δ_c values which were used to determine the stress intensification factor n from [2]

$$K = (E\sigma_y n\delta_c)^{1/2}$$

The values for K were taken from the J integral tests, σ_y values are 220 MN m^{-2} for the LA alloy and 240 MN m^{-2} for the HA alloy, and E is as above.

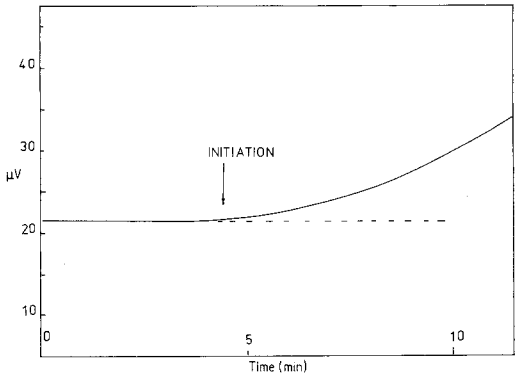

Figure 1 Probe voltage across notch versus time indicating initiation of fracture and crack growth.

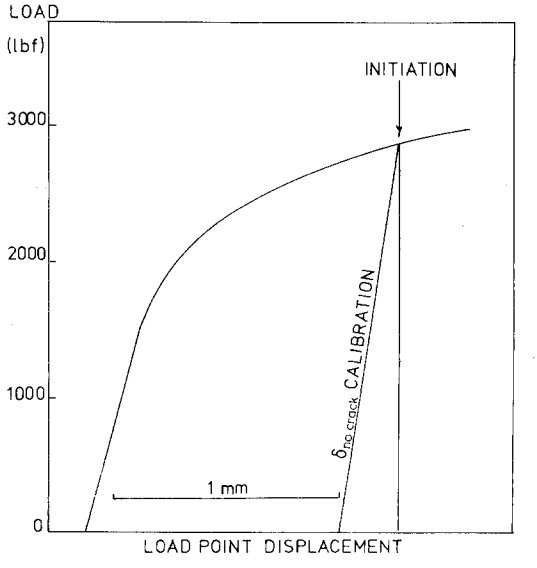

Figure 2 Load versus load-point displacement curve up to crack initiation beyond general yield.

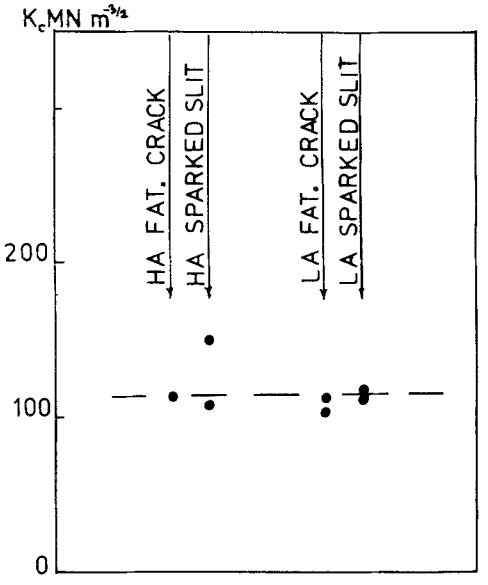

Figure 3 K_c values derived from *J*-integral values for alloys HA and LA in notched and fatigue cracked conditions.

3. Results

3.1. *J*-integral values for K_c

Fig. 2 shows a typical load versus load-point displacement to crack initiation with the area representing $\int_0^{\delta_{\text{no crack}}} P\mathrm{d}(\delta_{\text{no crack}})$ subtracted. The K_c values derived from these curves are shown in Fig. 3.

3.2. Crack opening displacements

Examples of the crack or slit tips before testing, and after crack initiation, are shown in Figs. 4 and 5. Average values for the critical COD and stress intensification *n* are shown in Table II.

TABLE II Critical COD values (mm)

Alloy	Notch Type	Av COD (mm)	*n*
LA	Spark Mach.	0.3	2.19
LA	Fat. Crack	0.4	1 41
HA	Spark Mach.	0.2	2.84
HA	Fat. Crack	0.3	1.45

3.3. Fracture surface

Nickel–aluminium bronzes are metallographically complex alloys containing α- and β-phases, and in addition about four morphological forms of the κ-phase [7, 8]. In the cast structure the distribution of α reflects a solid state transformation and so the actual locations of the dendritic as-cast β grain boundaries are not clearly apparent. In view of the high level of toughness of these alloys and the consequently large plastic zone preceding fracture, it would be expected that the 10 mm thick specimens would give plane stress shear fractures through the thickness, but in fact this did not occur. The fracture surfaces were predominantly normal to the tension stress giving the appearance of plane strain fractures. This fracture morphology must be dictated by metallographic structure. Figs. 6 and 7 shows, respectively, the fracture surface immedi-

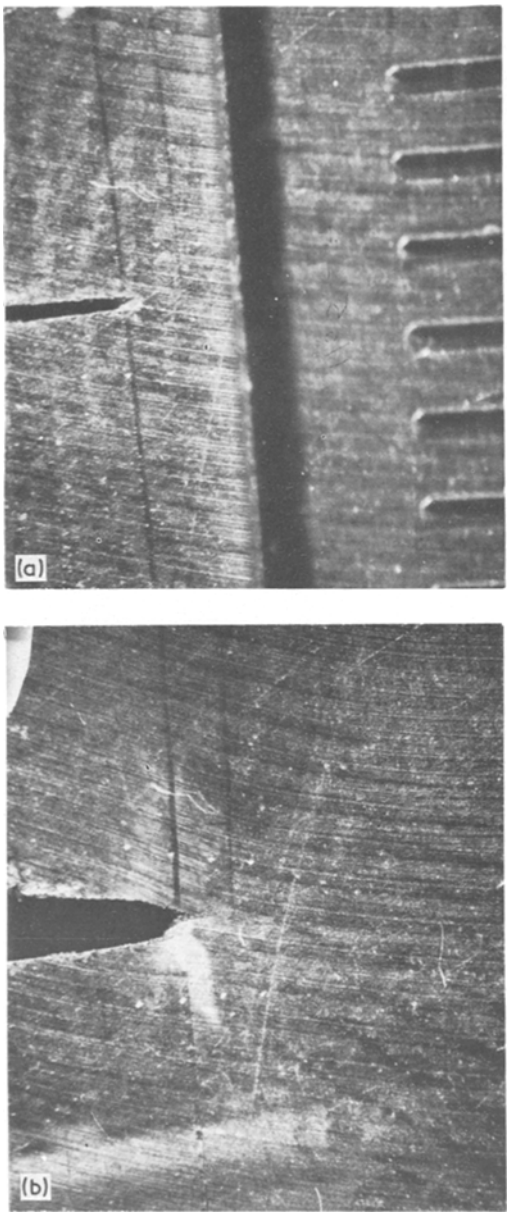

Figure 4 Notch tip (a) with micro-hardness indentations before testing, (b) immediately after initiation. × 13.

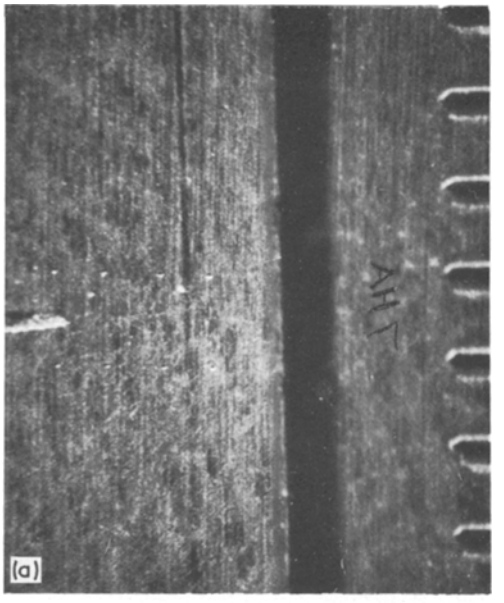

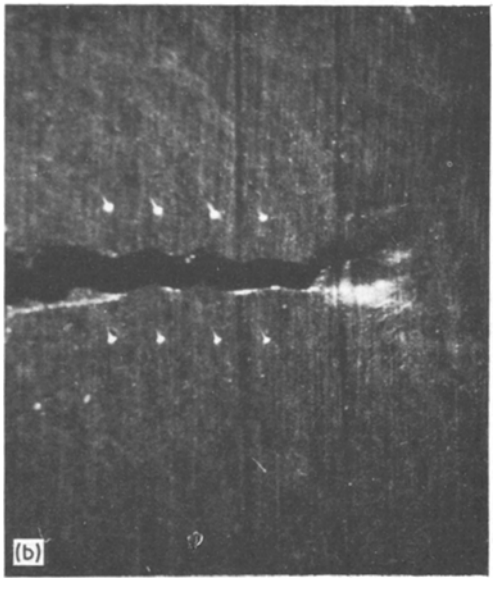

Figure 5 (a) Fatigue-cracked notch tip with micro-hardness indentations before testing. (b) Fatigue crack opening displacements immediately after initiation. × 13.

ately below a spark-machined slit, and the fracture surface in a pre-fatigue-cracked region. It seems likely that the structure sizes marked out in Figs. 6 and 7 correspond to the cast-grain size, and that the fracture path is dictated by intergranular fracture between cast grains.

Fig. 8 shows that the fracture was predominantly flat, but does reveal shear lips of a small size. These shear lips did not correspond in any way to the size (r_y) given by the equation [9]

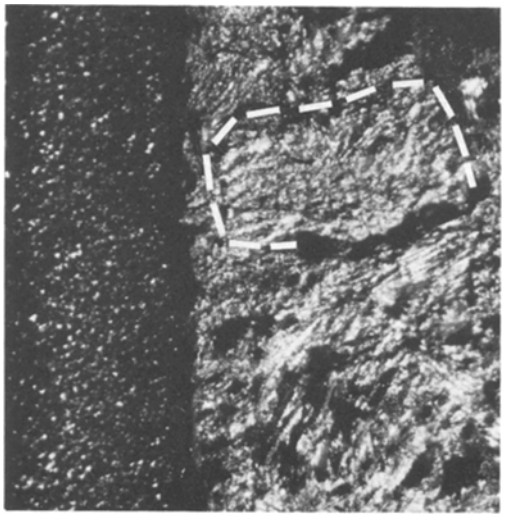

Figure 6 Fracture surface below spark-machined notch.

$$r_y = \frac{1}{2\pi}\left(\frac{K_c}{\sigma_y}\right)^2$$

In fact it appears that the shear lips are dictated by structure features of the alloy since they extended inwards about the distance proposed as the size of cast grains.

4. Discussion

There is no independent check on the K_c values derived from J_c values in Fig. 3, however similar testing on cast steels [10, 11] in which tests on larger specimens confirmed linear elastic K_c and

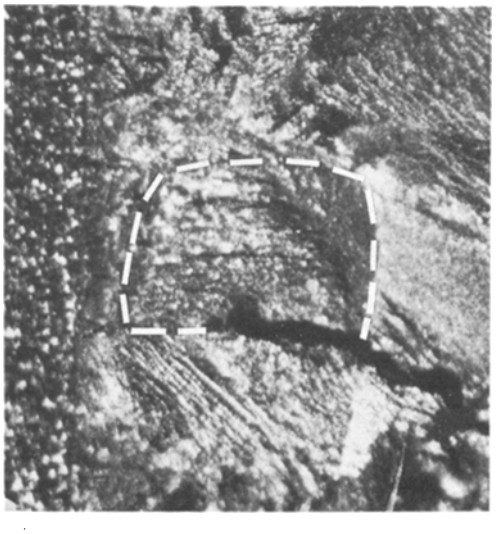

Figure 7 Fatigue crack surface below spark-machined notch.

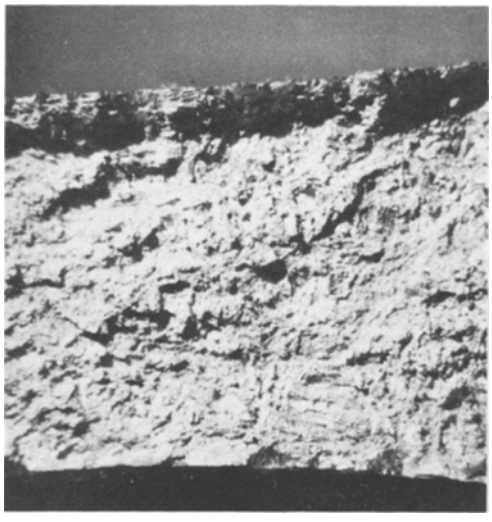

Figure 8 Shear lips and fracture surface.

K_{Ic} values, supports the derivation of K_c values. Further the values obtained are in substantial agreement with K_c values derived from a similar alloy in tube-burst experiments [12]. The COD values are too small to be sufficiently accurately measureable to give a conclusive check.

Typically the scatter in K_c values is quite large for cast materials [10, 11]. The values of Fig. 3 show such scatter, but it is clear that within this scatter band there is no significant difference between 0.2 mm wide slits and low stress fatigue cracks. This is particularly confirmed by the tests on the LA alloy. It should be emphasized that this equivalence can only be judged on small specimens using the J-integral values, and cannot be deduced from relative load levels at fracture since these are simply dictated by the general yield condition prevailing in both types of specimen at fracture initiation. Naturally in large structures which would fracture before general yield because of their geometry, the difference would, in fact, dictate the load level.

It seems highly likely that fracture paths and shear lips in these fracture tests are dictated entirely by the cast-grain size. Further work is proceeding to confirm this and to explore its implications.

Acknowledgement

This work has been carried out with the support of the Procurator Executive, Ministry of Defence and is published by permission of the controller, HMSO, holder of Crown Copyright. Any views expressed are those of the authors and do not necessarily represent those of the Department.

References

1. J. R. RICE, *J. Appl. Mech.* **35** (1968) 379.
2. A. A. WELLS, *Eng. Fract. Mechs.* **1** (1969) 399.
3. J. N. ROBINSON and A. S. TETELMAN, *ibid* 8 (1976) 301.
4. A. H. COTTRELL, *Proc. Roy. Soc.* **A285** (1965) 10.
5. J. R. RICE, P. C. PARIS and J. G. MERKLE, ASTM, STP No. 536 (1973).
6. BSI Methods for Crack Opening Displacement (COD) Testing, DD19: 1972.
7. P. WEILL-COULY and D. ARNAUD, *Fonderie* **28** (1973) 123.
8. E. A. CULPAN, G. ROSE and D. MOTH, unpublished work, (1976).
9. W. F. BROWN, and J. F. SRAWLEY, Plane Strain Cract Toughness Testing of High Strength Metallic Materials, ASTM, STP No. 410 (1966).
10. J. T. BARNBY and I. AL-DAIMALANI, *J. Mater. Sci.* **11** (1976) 1979.
11. *Idem, ibid* **11** (1976) 1989.
12. J. T. BARNBY, E. A. CULPAN, A. E. MORRIS, L. J. HUSSEY, M. S. ATHERTON and D. M. RAE, *Internat. J. Fracture* (to be published).

Received 30 November 1976 and accepted 25 January 1977.